Magnetic Excitations in a Weak-Stripe-Domain Structure: A 2D Dynamic Micromagnetic Approach

N. Vukadinovic and 0. Vacus
Dassault Aviation, 92 552 St-Cloud, France

M. Labrune
Laboratoire LPMTM, Institut Galilée, Université Paris-13, 93 430 Villetaneuse, France

0. Acher and D. Pain
CEA Le Ripault, LMMH, B.P. 16, 37 260 Monts, France
(Received 26 May 2000)

The high-frequency susceptibility spectra of ferromagnetic films supporting a weak-stripe-domain structure are computed using a 2D dynamic micromagnetic model that we have developed. The existence of multiple resonances resulting from the excitation of surface and volume modes is predicted. The main features of spectra (number of resonances, resonance frequencies, intensities, and linewidths) strongly depend on the equilibrium spin configuration and on the rf exciting field orientation. These theoretical results are successfully compared with zero-field microwave permeability measurements.

PACS numbers: 75.40.Gb, 75.60.Ch, 75.70.–i, 76.50.+g

The existence of equilibrium domain patterns in a wide class of physical systems has been recognized as a manifestation of modulated phases [1]. The periodic stripe domain structure observed in thin ferromagnetic films with a perpendicular magnetic anisotropy is a well-known example of such systems [2]. Among the various types of stripe domains [3], the so-called weak-stripe domains appearing in magnetic films with a low or intermediate perpendicular anisotropy ($Q < 1$, where Q is the quality factor defined as $Q = K_u/2\pi M_s^2$, with K_u the uniaxial anisotropy constant and M_s the saturation magnetization) represent a very attractive magnetic configuration. One of the main features is the existence of a critical thickness t_c; for low thicknesses $t < t_c$ the magnetization lies in the plane of the thin film, while, beyond t_c, the magnetization starts to oscillate out of the plane in a periodic manner, the half period being close to the film thickness. This second-order phase transition (the order parameter is the component of the magnetization normal to the film) was recently observed in Co [4] and FePd [5] thin films.

On the other hand, the dynamic response of stripe domains to a weak alternating magnetic field δh_{rf} was recently investigated in low or moderate Q-factor magnetic films [6–9]. As a result, microwave permeability spectra exhibiting multiple narrow resonances were reported in amorphous Co-Nb-Zr [6] and Co-Fe-Zr [7] thin films. In the same way, complicated ferromagnetic resonance (FMR) spectra in the unsaturated state with a series of peaks were also observed in Co [8] and FePd [9] thin films. First attempts for interpreting such magnetic excitations were performed with the help of an analytical model previously derived for the case of stripe domains in garnet films with alternatively up and down magnetization [10] (limit of a large Q value). It predicts the existence of two domain mode resonances (spin precession inside the domains with two types of phase relations between neighboring domains) and one Bloch domain wall resonance, but failed to account for the other magnetic excitations. To our knowledge, a quantitative model describing the whole magnetic excitation spectra in terms of mode positions, intensities, and linewidths was still lacking.

The purpose of this Letter is to investigate the frequency response of weak-stripe domains using a two-dimensional (2D) dynamic micromagnetic approach. Some typical spectra of dynamic susceptibility are predicted and correlated with the main features of the spin configuration in equilibrium. The great efficiency of such a method is demonstrated through a very good agreement with experimental permeability spectra (no fitting parameters).

The dynamic of stripe domains is considered from the micromagnetic point of view, where the magnetic medium is represented as a macroscopic continuum characterized by the magnetization vector $\boldsymbol{M}(\boldsymbol{r}, t)$ of constant modulus M_s [$\boldsymbol{M}(\boldsymbol{r}, t) = M_s \boldsymbol{m}(\boldsymbol{r}, t)$]. Let us consider a single period of the domain pattern; the x axis corresponds to the periodicity direction, the y axis is the film normal, and the z axis is oriented along the stripe direction. In the 2D micromagnetic simulations, the reduced magnetization $\boldsymbol{m}$ is assumed invariant along the z axis ($\boldsymbol{r}$ is restricted to vary in the x-y plane).

The dynamic micromagnetic simulations are performed in two steps.

Firstly, the equilibrium magnetization configuration is computed using a Labonte-Brown-type procedure [11,12]. A relaxation method is used iteratively in order to achieve the alignment of the magnetization vector along the effective field vector at each point of the discretization lattice in the cross section through the periodic cell (x-y plane). The effective field $\boldsymbol{H}_{\text{eff}}$ incorporates the contributions from the exchange, anisotropy, and demagnetizing

fields, $\boldsymbol{H}_{\text{eff}} = \boldsymbol{H}_{\text{exch}} + \boldsymbol{H}_{\text{anis}} + \boldsymbol{H}_{\text{demag}}$. This computation provides the equilibrium magnetization configuration $\boldsymbol{m}_{\text{eq}}(\boldsymbol{r})$, the equilibrium field $\boldsymbol{H}_{\text{eq}}(\boldsymbol{r}) = \boldsymbol{H}_{\text{eff}}[M_s \boldsymbol{m}_{\text{eq}}(\boldsymbol{r})]$ and the stable domain period P_0.

Secondly, the dynamic susceptibility is determined by computing the response $\delta\boldsymbol{m}(\boldsymbol{r}, t)$ of the magnetization configuration to a weak uniform magnetic excitation $\delta\boldsymbol{h}(t)$. The developed code for treating this problem is based on a method recently published [13] and is extended in order to take into account the periodic nature of the magnetization configuration. The time evolution of the magnetic configuration can be described by the Landau-Lifschitz-Gilbert equation:

$$\frac{d\boldsymbol{m}}{dt} = -|\gamma|\boldsymbol{m} \times \boldsymbol{H} + \alpha \boldsymbol{m} \times \frac{d\boldsymbol{m}}{dt}, \qquad (1)$$

where $\boldsymbol{m}$ can be expanded in the form $\boldsymbol{m}(\boldsymbol{r}, t) = \boldsymbol{m}_{\text{eq}}(\boldsymbol{r}) + \delta\boldsymbol{m}(\boldsymbol{r}, t)$, $\boldsymbol{H}$ represents the total magnetic field that can be written $\boldsymbol{H}(\boldsymbol{r}, t) = \boldsymbol{H}_{\text{eq}}(\boldsymbol{r}) + \delta\boldsymbol{h}(t) + \boldsymbol{H}_{\text{eff}}(\delta\boldsymbol{m})$, γ is the gyromagnetic ratio, and α is the Gilbert damping parameter. By considering a harmonic time dependence for $\delta\boldsymbol{h}$ and $\delta\boldsymbol{m}$ ($e^{i\omega t}$, ω is the angular frequency), and under the assumptions $|\delta\boldsymbol{h}| \ll |\boldsymbol{H}_{\text{eq}}(\boldsymbol{r})|$, $|\boldsymbol{H}_{\text{eff}}(\delta\boldsymbol{m})| \ll |\boldsymbol{H}_{\text{eq}}(\boldsymbol{r})|$, and $|\delta\boldsymbol{m}| \ll |\boldsymbol{m}_{\text{eq}}| = 1$, linearizing of Eq. (1) leads to the following linear system:

$$\left(-\frac{i\omega}{|\gamma|} I + D_2 - D_1 D_H\right)\delta\boldsymbol{m} = D_1 \delta\boldsymbol{h}, \qquad (2)$$

where I is the unit matrix and the matrices D_1, D_2, and D_H are defined, for any given vector $\boldsymbol{v}$, by

$$\begin{aligned} D_1\boldsymbol{v} &= \boldsymbol{m}_{\text{eq}} \times \boldsymbol{v}, \qquad D_H\boldsymbol{v} = \boldsymbol{H}_{\text{eff}}(\boldsymbol{v}), \\ D_2\boldsymbol{v} &= \left(\boldsymbol{H}_{\text{eq}}(\boldsymbol{r}) + \frac{i\alpha\omega}{|\gamma|}\boldsymbol{m}_{\text{eq}}\right) \times \boldsymbol{v}. \end{aligned} \qquad (3)$$

For a grid with N discretization points, $\delta\boldsymbol{m}$ and $\delta\boldsymbol{h}$ are $3N$ vectors and the linear dense system (2) is of size $3N \times 3N$. This system is solved for each frequency by using a direct method (Gauss factorization). The scalar dynamic susceptibility is then given by

$$\chi = \frac{1}{N}\sum_{i=1}^{N} \frac{\delta\boldsymbol{m}_i \cdot \delta\boldsymbol{h}_i}{|\delta\boldsymbol{h}_i|^2}. \qquad (4)$$

The computations were performed on a parallel computer with the treatment of one frequency per processor.

It was shown [2] that the zero-field micromagnetic state of thin films with a uniaxial perpendicular anisotropy may be represented in a phase diagram depending on two reduced parameters: the quality factor Q and, for instance, the ratio of the film thickness t to the exchange length $\Lambda = (A/2\pi M_s^2)^{1/2}$ with A the exchange constant. The reduced critical thickness for domain nucleation was computed using the procedure described in [2] and is displayed in the $(Q, t/\Lambda)$ plane in Fig. 1. In this phase diagram, two points located above the critical line were selected: point A ($Q = 0.5, t/\Lambda = 10$) and point B ($Q = 0.05, t/\Lambda = 60$), with a nearly constant ratio t/t_c.

The micromagnetic results concerning samples A and B are presented, respectively, in Figs. 2 and 3. The magnetic parameters are $4\pi M_s = 10\,000$ G, $A = 1 \times 10^{-6}$ erg/cm, $\gamma = 1.85 \times 10^7$ Oe^{-1} s^{-1}, $\alpha = 2.5 \times 10^{-2}$. The computations were performed on different discretization grids. As a conclusion, using a 64×31 grid leads to reliable results for both the static and the dynamic micromagnetic computations. The susceptibility spectra in the frequency range 100 MHz–30 GHz were first computed with a frequency step $\Delta f = 100$ MHz. A refinement ($\Delta f = 10$ MHz) was then performed around the detected resonance frequencies.

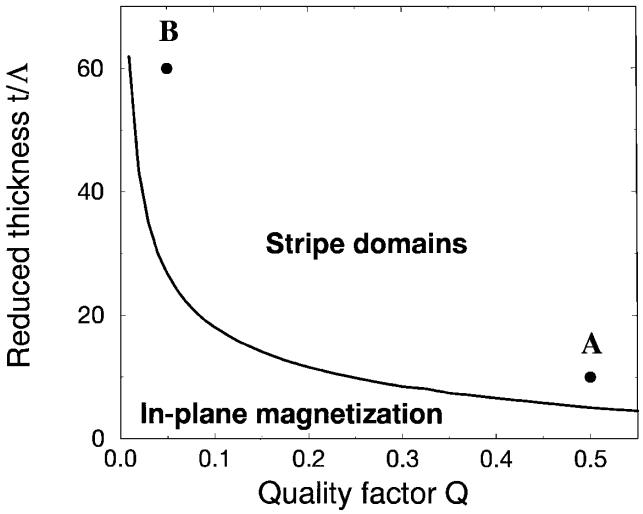

FIG. 1. Phase diagram in the $(Q, t/\Lambda)$ plane. The boundary line represents the reduced zero-field critical thickness t_c/Λ for domain nucleation. Coordinates are (0.5, 10) for point A and (0.05, 60) for point B.

Figure 2(a) exhibits the static magnetization configuration within one period for sample A. This configuration consists of an open flux pattern with large domains magnetized along the y direction separated by a Néel wall at the film surfaces and a Bloch wall at the film center. The film thickness is $t = 50$ nm, and the zero-field period corresponds to $P_0 = 134$ nm. The spectra of the dynamic susceptibility (imaginary part χ'') for the three main exciting directions δh_{rf} applied along the x axis (x configuration), y axis (y configuration), and z axis (z configuration) are displayed in Fig. 2(b). The results reveal the existence of multiple resonances whose numbers and positions depend on the direction of δh_{rf}. The largest response is obtained for the x configuration. The spectrum consists of one intensive peak labeled (1). It is also observed with a weaker intensity for the y configuration. In addition, a second resonance labeled (2) is clearly detected at a higher frequency. For the z configuration, the spectrum exhibits one intensive and two weaker resonances denoted, respectively, (3), (4) and (5). The resonance frequencies do not coincide with those pointed out for the two other exciting directions.

The existence of a nonuniform magnetic distribution and the strong inhomogeneity of the effective field make the description of the modes $\delta\boldsymbol{m}$ complicated. Figure 2(c) displays the modulus of $\delta\boldsymbol{m}$ within one period for peaks (1),

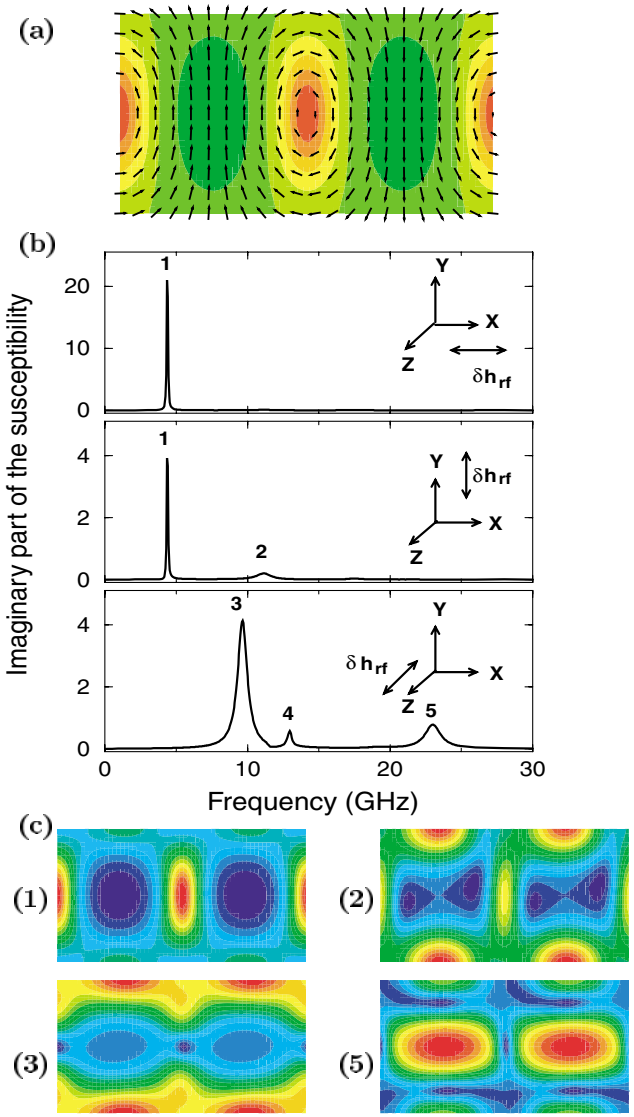

FIG. 2 (color). (a) Equilibrium magnetization configuration for sample A. The arrows represent the components of $\boldsymbol{M}$ in the plane of the figure. A color code is adopted for imaging the third component (high levels in red and low levels in green). (b) Corresponding dynamic susceptibility spectra. (c) $|\delta \boldsymbol{m}|$ for modes (1), (2), (3), and (5) (high levels in red and low levels in blue).

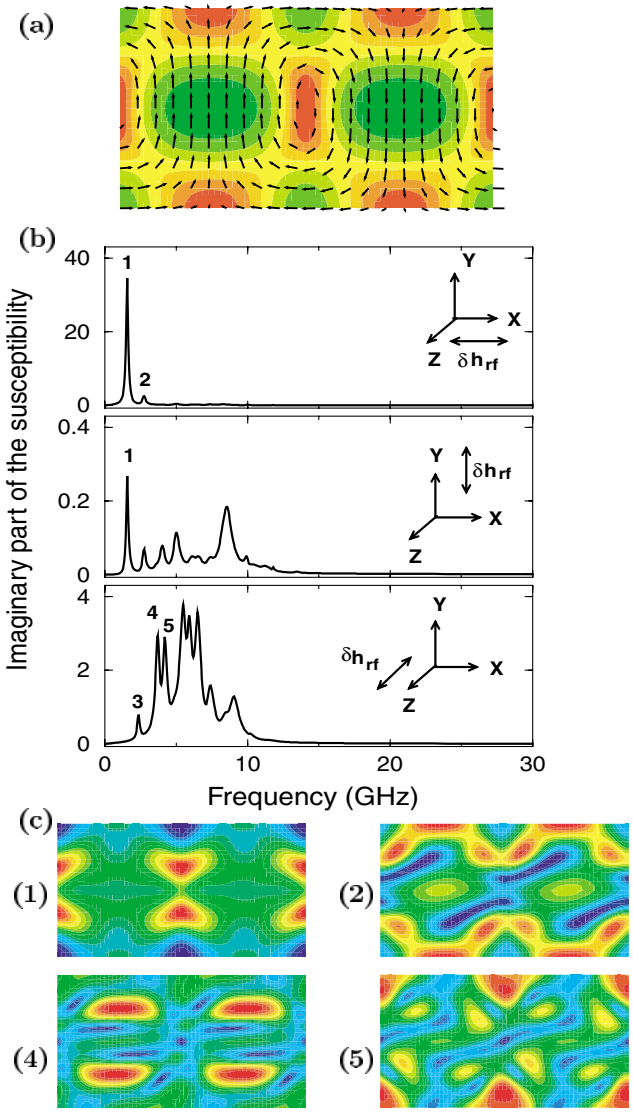

FIG. 3 (color). (a) Equilibrium magnetization configuration for sample B. (b) Corresponding dynamic susceptibility spectra. (c) $|\delta \boldsymbol{m}|$ for modes (1), (2), (4), and (5).

(2), (3), and (5). At each resonance frequency, this modulus is normalized by its maximal value. Mode (1) appears as a volume mode with maximum values of $|\delta \boldsymbol{m}|$ concentrated within Bloch-type domain walls. Nevertheless, as the area of domains is larger than the area of domain walls, their contributions to susceptibility are comparable. For mode (2), the higher values of $|\delta \boldsymbol{m}|$ are located at surfaces of domains and within Bloch-type domain walls. Mode (3) is a surface mode while mode (5) is a volume mode with maximum values of $|\delta \boldsymbol{m}|$ at the center of the domains.

The static magnetization configuration within one period for sample B is depicted in Fig. 3(a). The configuration approaches a Landau-Lifschitz structure with domains magnetized along the y direction separated by a Bloch-type domain wall at the film center and closure domains at the film surfaces ensuring a quasiflux closed pattern. The film thickness is $t = 300$ nm, and the zero-field period corresponds to $P_0 = 475$ nm. The spectra of dynamic susceptibility for the three exciting directions are reported in Fig. 3(b). The largest susceptibility response is obtained for the x configuration. The spectrum consists of one intensive peak labeled (1) and a subsidiary one labeled (2) of weak intensity and located at a higher frequency. With respect to sample A, the peak (1) appears at a lower frequency and its intensity is increased. The spectra for the y and the z configurations are respectively 2 and 1 orders of magnitude lower than that for the x configuration and, moreover, very different from those reported for sample A. Instead of well-located resonances, an extended frequency response (1–15 GHz) with a complicated fine-structure is observed. This behavior is related to the large distribution

of the dynamic effective field [$\boldsymbol{H}_{\text{eff}}(\delta \boldsymbol{m})$ term] occurring in low-Q thin films.

Some modes are shown in Fig. 3(c). Mode (1) appears as a volume mode with the maximum of $|\delta \boldsymbol{m}|$ concentrated near the domain walls. Mode (2) exhibits high values of $|\delta \boldsymbol{m}|$ at surfaces of domains and on the boundary lines separating domains and closure domains. Mode (4) is a volume mode, the higher values of $|\delta \boldsymbol{m}|$ correspond to a part of the domains. For mode (5), the large variations of $|\delta \boldsymbol{m}|$ are mainly located within the closure domains; this mode looks like the flux closed cap mode (out of phase precession) predicted in [8].

The theoretical results concerning point B have been compared with experimental data obtained from microwave permeability measurements using a permeameter described elsewhere [14]. The selected sample corresponds to an amorphous $Co_{63}Fe_{26}Zr_{11}$ thin film whose weak-stripe-domain structure was imaged using a magnetic force microscopy ability. This film exhibits a biaxial anisotropy with an in-plane component K_p and a perpendicular component K_u. The structural and magnetic properties of this film were previously reported [15]. In the phase diagram, this film is located in the vicinity of sample B ($Q = 0.05$, $t/\Lambda \simeq 68$). The in-plane microwave permeability (imaginary part, $\mu'' = 4\pi\chi''$) recorded in the 10 MHz–6 GHz frequency range along the in-plane hard axis x (x configuration) and the easy axis z (z configuration) is reported, respectively, in Figs. 4(a) and 4(b). The experimental spectra are characterized by the existence of multiple well-resolved resonances. Without any fitting parameters, a very good agreement is found between the experimental and theoretical spectra (Fig. 4). The only noticeable difference occurs for the third excitation in Fig. 4(b). This could be explained by the effect of eddy currents. Typically, the skin depth δ can be estimated to be 450 nm at 5 GHz leading to the ratio $t/\delta \simeq 2/3$. It means that the exciting magnetic field is slightly inhomogeneous along the film thickness. Since mode (5) is a surface mode [Fig. 3(c)], the exciting field can favor the coupling with the magnetic moments located at the upper interface with respect to those at the lower interface, resulting in an inhomogeneous broadening of the experimental line.

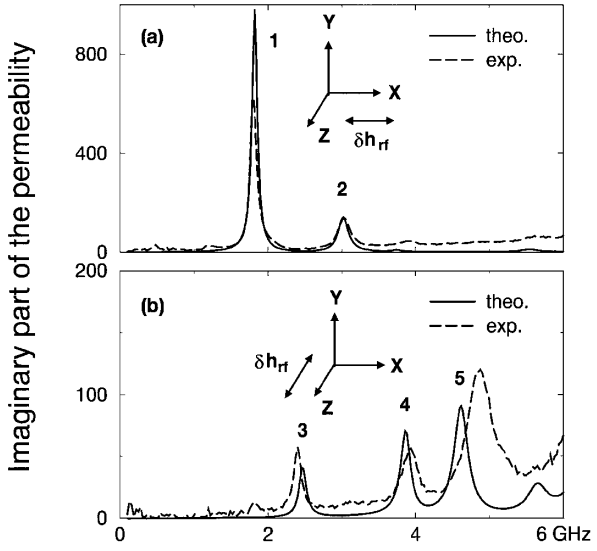

FIG. 4. Comparison between the theoretical (solid line) and experimental (dashed line) permeability spectra; (a) δh_{rf} along the x axis, (b) δh_{rf} along the z axis. The film is a 300 nm amorphous $Co_{63}Fe_{26}Zr_{11}$ monolayer. The zero-field stripe period is equal to $P_0 = 500$ nm. The magnetic parameters are $4\pi M_s = 12\,000$ G, $K_p = 1.6 \times 10^4$ erg/cm^3, $K_u = 2.3 \times 10^5$ erg/cm^3, $A = 1.1 \times 10^{-6}$ erg/cm, g factor = 2.2, and $\alpha = 1.2 \times 10^{-2}$.

To summarize, a 2D-dynamic micromagnetic code has been developed and used to analyze the magnetic excitations of perpendicular anisotropy thin films with stripe domains. The following results have been observed: (i) the theoretical dynamic susceptibility spectra reveal multiple resonances whose number, resonance frequencies, intensities, and linewidths depend on the static magnetization configuration and the direction of the rf exciting field, (ii) the physical origin of observed magnetic excitations has been explained in terms of surface and volume modes of stripe domains, (iii) these theoretical predictions have been compared successfully with experimental zero-field microwave permeability spectra. The ability of dynamic micromagnetic simulations for interpreting high-frequency responses of thin magnetic films has been established. Further comparisons with FMR data will be published in a forthcoming article.

[1] M. Seul and D. Andelman, Science **267**, 476 (1995).
[2] A. Hubert and R. Schaefer, *Magnetic Domains* (Springer, New York, 1998).
[3] M. Labrune and J. Miltat, J. Appl. Phys. **75**, 2156 (1994).
[4] M. Hehn, S. Padovani, K. Ounadjela, and J. P. Bucher, Phys. Rev. B **54**, 3428 (1996).
[5] V. Gehanno, R. Hoffmann, Y. Samson, A. Marty, and S. Auffret, Eur. Phys. J. B **10**, 457 (1999).
[6] Y. Shimada, M. Shimoda, and O. Kitakami, Jpn. J. Appl. Phys. **34**, 4786 (1995).
[7] O. Acher, C. Boscher, B. Brulé, G. Perrin, N. Vukadinovic, G. Suran, and H. Joinsten, J. Appl. Phys. **81**, 4057 (1997).
[8] U. Ebels, P. E. Wigen, and K. Ounadjela, Europhys. Lett. **46**, 94 (1999).
[9] N. Vukadinovic, H. Le Gall, J. Ben Youssef, V. Gehanno, A. Marty, Y. Samson, and B. Gilles, Eur. Phys. J. B **13**, 445 (2000).
[10] M. Ramesh and P. E. Wigen, J. Magn. Magn. Mater. **74**, 123 (1988).
[11] A. E. Labonte, J. Appl. Phys. **40**, 2450 (1969).
[12] M. Labrune and J. Miltat, IEEE Trans. Magn. **MAG-26**, 1521 (1990).
[13] S. Labbé and P. Y. Bertin, J. Magn. Magn. Mater. **206**, 93 (1999).
[14] D. Pain, M. Ledieu, O. Acher, A. L. Adenot, and F. Duverger, J. Appl. Phys. **85**, 5151 (1999).
[15] G. Suran, M. Naili, H. Niedoba, O. Acher and D. Pain, J. Magn. Magn. Mater. **192**, 443 (1999).